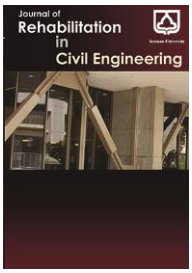

Journal homepage: http://civiljournal.semnan.ac.ir/

The Effect of Opening on Stiffness and Strength of Infilled Steel Frames

Mostafa Abbasnejadfard[1*] and Masood Farzam[2]
1. M.Sc., Structural Engineering, University of Tabriz, Tabriz, Iran
2. Assistant Professor, University of Tabriz, Tabriz, Iran

Corresponding author: mostafaabbasnejad@gmail.com

ARTICLE INFO

Article history:
Received: 01 October 2016
Accepted: 17 November 2016

Keywords:
Infill,
Opening,
ATENA,
L-shaped strengthening,
Hollow clay tile.

ABSTRACT

Infilled walls are the major non-structural elements which have significant effects on the seismic behavior of structures. The shape and strength of the brick elements are the main parameters affect the strength of the walls. In addition existence of openings may have a reduction effect. To increase the strength of the wall and to improve its behavior, the borders of the openings may be strengthened. In this paper, a one-story one-bay infilled steel frame which have been experimentally tested is modeled numerically and analyzed by commercial software ATENA. The wall was made of hollow clay tiles and cement mortar. The infilled frame was modeled under monotonically increasing loads until the failure. The numerical model is verified by comparing the cracking shape and the load-drift curves of the experimental and numerical models. Based on this numerical model, investigations on the effect of openings with different size and locations on the in-plane behavior of the walls are conducted. The effect of the strengthening of opening borders is probed additionally. Observations showed that the effect of openings is negligible for the opening with less than 10% area of the wall. In other cases, the lateral strength of the infilled frame reduced by 20-80% based on the size and location of the openings. The strengthening of all borders of openings with L-shaped steel angels can improve the behavior. The arrangement of these border elements may be changed to show better performance.

1. Introduction

Masonry infilled frames can be found in many parts of the world. There is a lack of structural design standards for masonry infill walls since they are normally treated as non-structural components. However, they will interact with the bounding frame in the event of an earthquake. The ability to assess the seismic performance of these structures is of great importance from the standpoint of hazard mitigation and life safety

[1]. It has been reported that addition of masonry walls in steel or RC frames raises the in-plane stiffness and strength of the structure because of the infill-frame interaction. The resulting system is referred to as an infilled frame, and it acts significantly differently from each constitutive parts (frame and infill wall), which highly affects the dynamic response of the structure [2].

Extensive experimental and analytical studies have been conducted on the behavior of masonry infills under lateral loads [3].Moghadam [4] conducted an experimental study on reinforced infills enclosed in a steel frame. Moghadam et al. [5] conducted an experimental study on masonry walls in reinforced concrete frames with different size in the presence or absence of horizontal bars. Doudoumis [6] used an accurate finite element model to investigate the effect of block contact, mesh density and beam-column stiffness ratio on the infilled frame behavior .Khanmohammadi et al.[1] conducted an experimental investigation on a one-story, one-bay infilled steel frame made by hollow clay tiles under cyclic loading. Koutromanos et al. [7] used smeared-crack continuum elements with cohesive crack interface elements to describe the salient features of the inelastic behavior of RC frame. The inelastic seismic response of a three-story, two-bay frame tested on shake table, successfully simulated by a finite element method. The results showed that even though infill walls were considered as non-structural element in design, they can contribute to seismic resistance of a structure significantly. Markulak et al. [8] investigated the behavior of nine one-bay, one-story steel frames infilled with different masonry under cyclic load. Stiffness, strength and dissipation capacity was increased in campier whit bare frame. Jazany et al. [9] studied the effect of masonry-infill on the seismic performance of concentrically braced frames (CBF) experimentally and analytically. Results inducted that the presence of masonry-infill increased the lateral stiffness and strength of the CBF by 33% and 41% respectively. Fiore et al. [10] proposed two equivalent strut models for simulating the complex behavior of infilled frame under the lateral load. This investigation underlined the necessity to take into account not only the stiffening contribution of panels, but also the positive contribution to bending moment and negative effect due to non-negligible increments in proximity of structures nodes.

An opening in an infill changes the behavior of building and decreases the lateral strength and effective stiffness of infill. Despite numerous investigations and experiments on infills, there is still uncertainty about the behavior of infills with openings. Moslem et al. [11] expressed that the presence of openings in infills led to 40% decrease in lateral stiffness. The presence of opening led to brittle failure of infills. Mohammadi and Nikfar [2] studied six empirical formulas for reduction factor (R_f) for consideration of the effect of opening on strength of masonry-infill frames. the result showed that the equation proposed by AL Chaar et al. [12] estimated both the initial stiffness and ultimate strength of the specimens with window and door openings more accurately than the others. More investigation demonstrated that the R_f for ultimate strength in AL Chaar et al. [12] equation depended on frame material. In contrast initial stiffness-reduction factor was independent of the frame material. Liu et al. [13] tested thirteen concrete masonry infilled steel frames to investigate the behavior and capacity of such systems under in-plane lateral loading and combined lateral and axial load. They expressed that reduction in the stiffness and ultimate load was not in proportion to the area of the opening. For low axial load level, the presence of axial load notably increased the ultimate load of infilled frame. Axial load effect on the stiffness of fully grouted infill was more significant than the partially grouted infills.

According to Kakaletsis and Karayannis [14] studied the effect of door and window openings on hysteresis characteristics of infills enclosed in reinforced concrete frames to determine the advantages and disadvantages of doors and windows of various sizes. Kakaletsis and Karayannis [15] experimentally studied the effect of opening shape and size on the seismic behavior of eight reinforced concrete frames. Their results indicated that openings with

different sizes and shapes decreased the strength and stiffness. They also proposed a load-displacement model for nonlinear analysis of the infills with openings. Chen et al. [16] developed a finite element model to study the effect of opening size and location on the stiffness and strength of masonry-infills bounded by steel frames. They expressed that an increase in the opening area decreased both strength and stiffness of infills. However, the rate of this reduction was associated with the location of the opening. Opening offsets away from the loaded side had lesser reduction effect. The reduction factor (R_f) had an approximately linear relationship with opening offset to length of masonry-infill ratio (e_c/L) and a parabolic relation with opening area to masonry-infill ratio ($A_\circ/A_p$). Mallick and Garge [17] investigated the effect of the opening location at the lateral stiffness in the presence of steel angle ties. According to the results, when an opening was installed at both ends of the diagonal of an infill in the absence of steel angle ties, the strength and stiffness of the frame respectively decreased by 75% and 85-90% compared with an infill without opening. Opening in the middle of infilled frame had minimum influence on its behavior.

In this study, one specimen that tested by Khanmohammadi et al [1] were modeled and calibrated with the finite element program ATENA [18]. To investigate the effect of opening on the stiffness and strength of infills, thirteen types of opening infilled frame with different size and positions were modeled. to examine the effect of opening shape, infills with window and door openings were studied. Finally, three models with an opening in the center of wall with horizontal, vertical and window shaped steel angle ties were analyzed. The results were compared with the data obtained from sample without opening.

2. Modeling

2.1. Geometry of specimens and material properties

The specimens were tested by Khanmohammadi et al. [1] were prepared with a scale of 1:2. Table 1 shows the wall dimensions and characteristics. In this study, these specimens were modeled and investigated analytically.

In this study, frames have two hinged joints at the bottom of columns. There are two other hinges in the beam-column connection. The surrounding frame only serves as a boundary element and has negligible stiffness and strength [1].

Table 1. Properties of test specimen [1]

Specific	Quantity	Unit
Length	1810	mm
Height	1440	mm
Height of loading point	1370	mm
Average thickness	120	mm
Height to Length ratio	0.79	-
Number of brick rows	6.5	-

A three dimension nonlinear material was used in order to simulate the brick units in ATENA. The theoretical backgrounds of material behavior used in modeling of specimens are described in following [19].

The used biaxial stress failure criterion was based on Kupfer et al. [20] as shown in Fig. 1. In the compression-compression stress state the failure function is:

$$f'^{ef}_c = \frac{1+3.65a}{(1+a)^2} f'_c, a = \frac{\sigma_{c1}}{\sigma_{c2}} \quad (1)$$

Where σ_{1c}, σ_{2c} are the principal stresses in concrete and f'_c is the uniaxial cylinder strength. In the tension-tension state, the tensile strength is constant and equal to the uniaxial tensile strength f'_t. In the tension-compression state, the tensile strength is reduced by the Eq.2.

$$f'^{ef}_t = r_{et} f'_t \quad (2)$$

$$r_{et} = 1 - 0.8\frac{\sigma_{c2}}{f'_c} \quad (3)$$

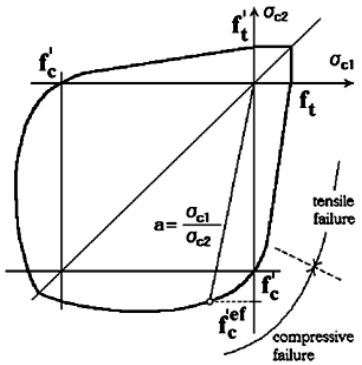

Fig. 1: Biaxial failure function for brick [19]

The nonlinear behavior of Brick in the biaxial stress state is described by means of the so-called effective stress σ_c^{ef}, and the equivalent uniaxial strain ε^{eq}. The effective stress is in most cases a principal stress.

The equivalent uniaxial strain is introduced in order to eliminate the Poisson's effect in the plane stress state.

$$\varepsilon^{eq} = \frac{\sigma_{ci}}{E_{ci}} \qquad (4)$$

The equivalent uniaxial strain can be considered as the strain, that would be produced by the stress σ_{ci} in a uniaxial test with modulus E_{ci} associated with the direction *i*.

Fictitious crack model based on a crack-opening law and fracture energy is suitable for modeling of crack propagation. It is used in combination with the crack band. Exponential Crack Opening Law which is one of the softening models was derived by Hordijk [21] (Eq.5).

$$\frac{\sigma}{f_t^{ef}} = \left\{1+(C_1\frac{w}{w_c})^3\right\}exp(-C_2\frac{w}{w_c}) - \frac{w}{w_c}(1+C_1^3)^2 exp(-C_2)$$

$$w_c = 5.14\frac{G_f}{f_t^{ef}} \qquad (5, 6)$$

In Eq.5, w is the crack opening, w_c is the crack opening at the complete release of stress (Eq.6), σ is the normal stress in the crack (crack cohesion). Values of the constants are, c_1=3, c_2=6.93. G_f is the fracture energy needed to create a unit area of stress-free crack, f_t^{ef} is the effective tensile strength derived from a failure function. The mentioned parameters and the size of bricks are presented in Table 2 and 3.

Table 2 Properties of brick units

Specific	Amount	Unit
Length	251.1	mm
Height	96.2	mm
Thickness	197.3	mm
Young's modulus of masonry brick (E_b)	300	MPa
brick compressive strength ($f_b^{'}$)	6.28	MPa
brick tensile strength (f_t)	0.811	MPa
Specific fracture energy (G_{fi})	1.849×10^{-5}	MN/m
Critical fictitious compression (w_d)	-5×10^{-4}	m
Plastic strain at compressive strength (ε^{eq})	-3.34×10^{-4}	-

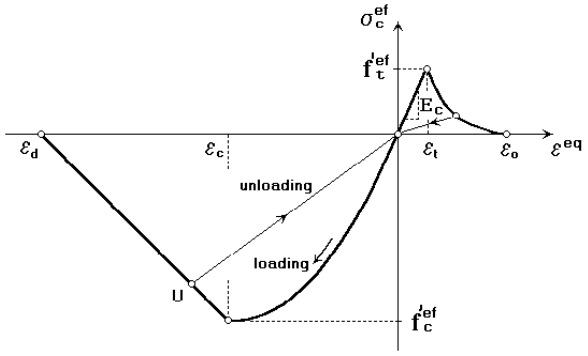

Fig. 2: Uniaxial stress-strain law for brick [19]

Table 3 Properties of surrounding frame

Specific	Amount	Unit
Young's modulus of steel (E_s)	2.1×10^6	GPa
Poisson's ratio of steel (υ_s)	0.15	-

Mortar is used in horizontal layers and there is no mortar between vertical layers of bricks. Fig. 3 shows mortar modeling by ATENA. the joint is modeled as an interface with zero thickness, in analogy .In this approach, fictitious expanded block dimensions are used that are of the same size as the original dimensions plus the real joint thickness as shown in Fig. 3. This is a conventional way for modeling the mortar layer. By Defining an interface material, mortar properties such as cohesion and stiffness are applied into the interface according to table 4.

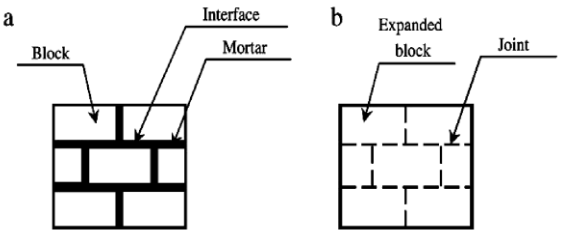

Fig. 3: Micro-modeling strategies for masonry walls: (a) detailed; and (b) semi-detailed [22]

The interface material model can be used to simulate contact between two materials such as for instance a construction joint between two concrete segments or a contact between foundation and concrete structure. The interface material is based at Mohr-Coulomb criterion with tension cut off. The constitutive relation for a general three-dimensional case is given in terms of tractions on interface planes and relative sliding and opening displacements.

$$\begin{Bmatrix} \tau_1 \\ \tau_2 \\ \sigma \end{Bmatrix} = \begin{bmatrix} k_{tt} & 0 & 0 \\ 0 & k_{tt} & 0 \\ 0 & 0 & k_{nn} \end{bmatrix} \begin{Bmatrix} \Delta v_1 \\ \Delta v_2 \\ \Delta u \end{Bmatrix} \qquad (7)$$

The initial failure surface corresponds to Mohr-Coulomb condition with tension cut-off. After stresses violate this condition, this surface collapses to a residual surface which corresponds to dry friction (Fig. 4).

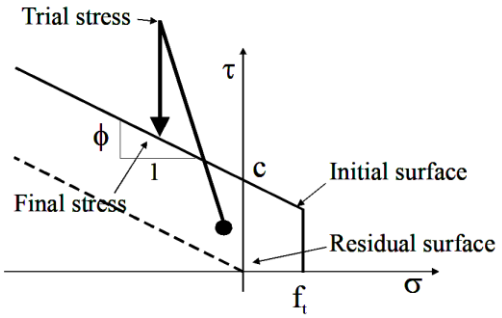

Fig. 4: Failure surface for interface elements [19]

The K_{nn}, K_{tt} denote the initial elastic normal and shear stiffness respectively. Typically for zero thickness interfaces, values of these parameters correspond to a high penalty number. It is recommended not to use extremely high values as this may result in numerical instabilities. It is recommended to estimate the stiffness value using the following formulas:

$$K_{tt} = \frac{E}{t} \qquad (8)$$

$$K_{nn} = \frac{G}{t} \qquad (9)$$

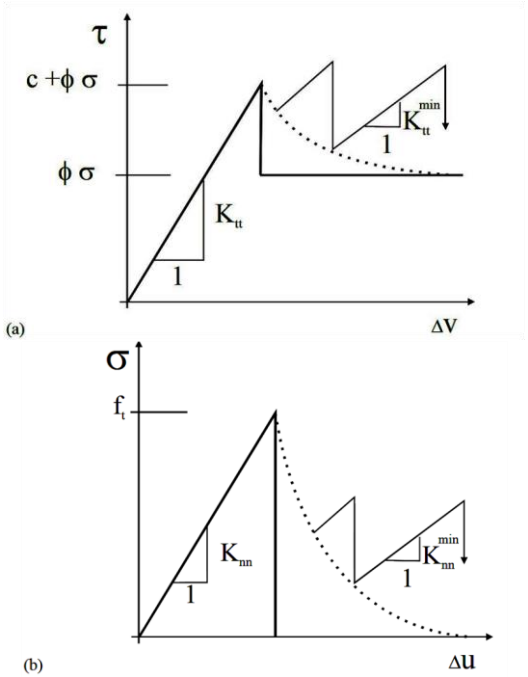

Fig. 5: Typical interface model behavior in shear (a) and tension (b) [19].

Where E, G and is minimal elastic modulus and shear modulus respectively of the surrounding material. *t* is the width of the interface zone.

Table 4. Properties of mortar

Specific	Amount	Unit
Normal stiffness (K_{nn})	5×10^5	MN/m^3
Shear stiffness (K_{tt})	5×10^5	MN/m^3
Tensile strength of mortar (f_m)	0.1	MPa
Cohesion (C)	0.31	MPa
Friction coefficient (υ_c)	0.79	-

2.2. Loading properties

The modeled specimen was placed under monotonic displacement-controlled loading. The load was increased with a rate of 0.2 mm per step and continued to a displacement of 4 cm. The pressure load was applied at the center of the plate attached to the column at a height of 137 cm.

2.3. Finite element (FE) meshes

FE mesh tool serves to define parameters for generation of finite element mesh. Brick meshes are possible for prismatic macro-elements. Brick meshes were used for Masonry units in 12.5 cm dimension equal to half size of brick units. Mesh length were refined for frame elements. (Fig. 6)

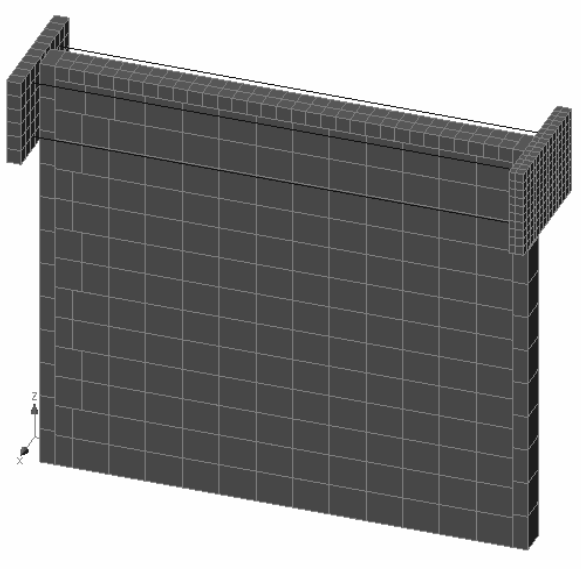

Fig. 6: Finite element mesh of numerical model

3. Comparison of analytical and experimental results

3.1. Infill failure mode

Crack patterns, tensile contours and deformation shape are illustrated in Fig. 7. With increasing the displacement; the gaps between bricks and frame were increased. At the drift of 0.05, the first crack occurred in the left corner near the loading point. In this step, separation occurred between the bricks, but no sliding observed. At the drift of 0.21, the maximum strength observed equal to 24 KN. From this point, crushing was increased and bricks began to slide. It seems that as the corner crushed, wall strength was significantly decreased.

In the final step, horizontal and diagonal gap developed and three parallel diagonal cracks were formed at the left side. The brick at the upper corner of the wall was completely crushed and the cracks in the bricks reached to the fourth rows. Bricks at the right side were less possible to failure because of the remoteness of the loading point. Thus, diagonal sliding and cracks in this area was little.

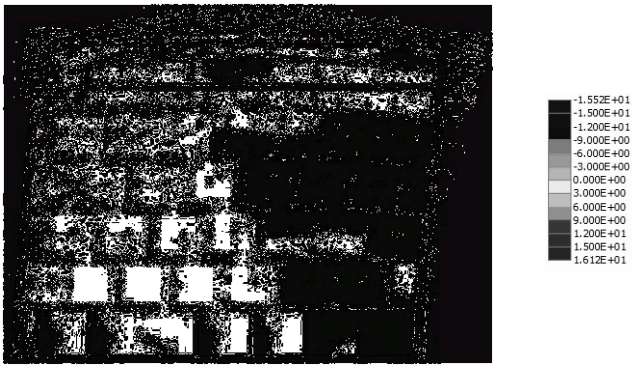

Fig. 7: Tensile contours (MPa), Crack patterns and deformed geometry of infilled wall without opening

3.2. Model validation

Fig. 8 illustrates the load–displacement diagrams of the experimental test and the numerical analysis. Table 5 lists the drift corresponding to the peak, maximum strength and stiffness of specimens and differences between the experimental and numerical results. The agreement between experimental and numerical responses is satisfactory with an error of 3.6% for maximum strength and 12.7% for initial stiffness of specimens.

Table 5. Maximum strength and stiffness of experimental and numerical specimens

Specific	Experimental	Numerical	Deference (%)
Maximum strength (KN)	24.9	24	3.6
Stiffness (KN/m)	9.565	8.342	12.7
Drift of Maximum strength	0.19	0.21	9.5

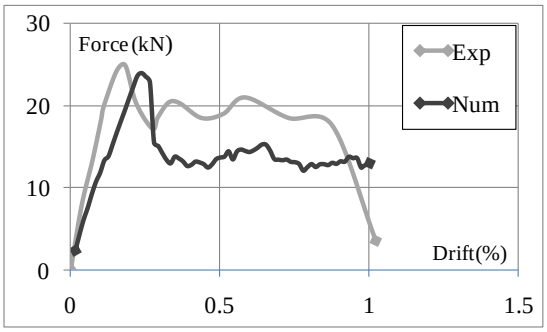

Fig. 8: Lateral load–displacement diagrams for experimental and numerical specimens

Fig.9 shows failure modes of the numerical and experimental specimens. Comparison shows a good agreement between the failure modes of experimental specimens and the modeled walls. As mentioned, corner cracking and diagonal and horizontal sliding are dominant failure mode and this could be an indicative of model accuracy.

4. The effect of opening on the wall behavior

After model verification, the effect of opening location and percentage on the strength and lateral stiffness of the infills were investigated.
To evaluate the effect of opening location, openings were created in the top-left, middle, bottom-right, bottom-left and top-right corners of the wall which abbreviated by TL, CO, BR, BL, TR and shown schematically in Fig. 10.

4.1. Central Opening (CO)

Table 6 represents the symbol and properties of four specimens with opening at the middle range of the infill.
The cracking and deformation patterns of four specimens are similar. Fig.11 shows load-displacement diagrams for four specimens with central opening. The diagrams were compared with load-displacement diagram of specimen without opening. The opening reduces the strength and stiffness of the wall and frame. Fig.12 illustrates the tensile contours, crack patterns and deformed geometry of CO4 specimen.

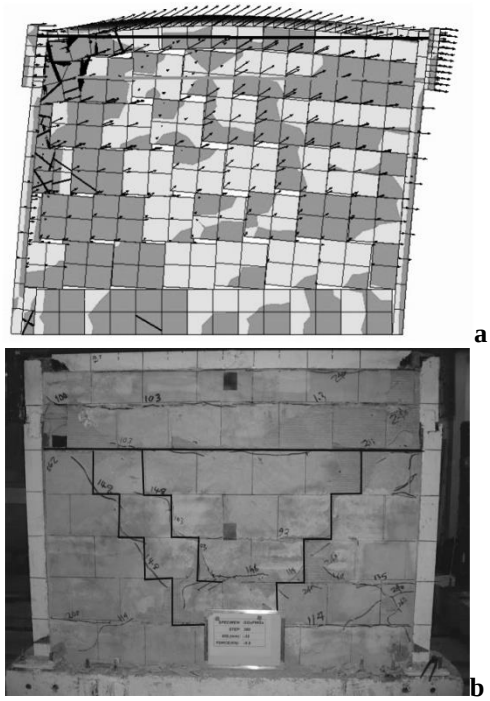

a

b

Fig. 9: Ultimate failure modes of; (a) numerical and (b) experimental [1] specimens.

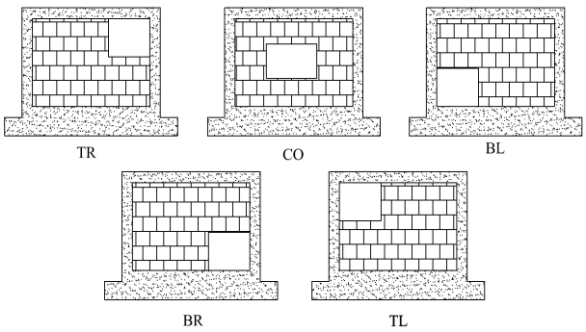

Fig. 10 Position of opening in the test specimens

Table 6. Properties of specimens with opening at the central part of the infill(CO)

Specimen Symbol	Infill Dimensions (cm)	Opening Dimensions (cm)	Opening Dimensions ratio	Opening Percentage (%)
CO 1	181×137	50×44	1.13	8.87
CO 2	181×137	75×66	1.13	20
CO 3	181×137	100×77	1.29	31.05
CO 4	181×137	100×88	1.13	35.5

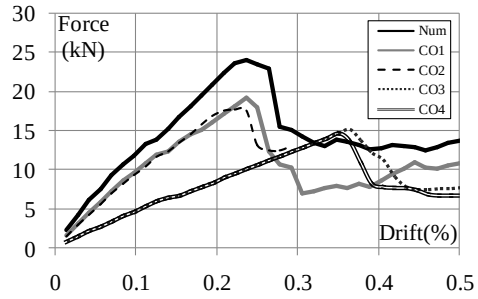

Fig.11: load-displacement diagrams for central opening infilled specimens

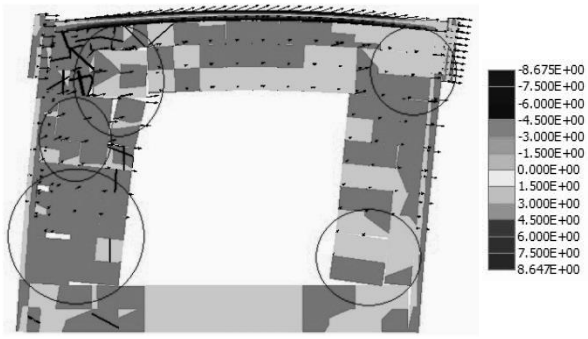

Fig .12: Tensile contours (MPa), Crack patterns and deformed geometry of central opening infilled wall (CO4)

The wall strength decreases with increasing the opening area due to reduced contact between the bricks in the center of the wall. With the formation of cracks, the factor that resisted against lateral load is further weakened. Thus, because of the fastening between the bricks, shear strength of the wall reduced by applying the lateral load. As a result, the wall can be failed under lower loads than without opening sample. Fig.13 shows the relationship between the opening percentage and ultimate strength of infilles. It should be noted that opening length has a greater impact on the stiffness than other dimensions.

FEMA-356 [23] proposed the following equation to calculate wall stiffness:

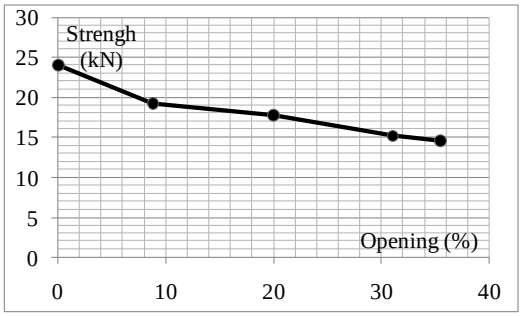

Fig.13: Relationship between the opening percentage and ultimate strength of CO infilled wall

$$k = \frac{1}{\frac{h_{eff}^3}{3I_g E_m} + \frac{h_{eff}}{A_v G_m}} \quad (10)$$

Where h_{eff} is wall height, A_v shear cross-sectional area, I_g moment of inertia of the uncracked section, E_m masonry elasticity modulus and G_m is the shear modulus of elasticity. According to the above equation, the opening leads to a decrease in the cross-sectional area and moment of inertia of the wall and thus the stiffness of wall is reduced. It should be noted that opening length has a greater impact on the stiffness than other dimensions.

4.2. Opening at the top-left of the infill (TL)

Table 7 represents the symbol and properties of two specimens with opening at the top-left of the infill. Fig.14 shows load-displacement diagrams for two TL specimens. Due to the absence of a wall in the corner of the frame and because of beam-column hinge joint, there is no element to resist against the lateral load. Thus, a large displacement occurs between the bricks and the wall is not able to bear the load. Fig. 15 shows the crack patterns and deformed geometry of the TL 2 specimen.

Table7 Properties of specimens with opening at the top-left of the infill (TL)				
Specimen Symbol	Infill Dimensions (cm)	Opening Dimensions (cm)	Opening Dimensions ratio	Opening Percentage (%)
TL 1	181×137	50×44	1.25	8.87
TL 2	181×137	75×66	1.13	20

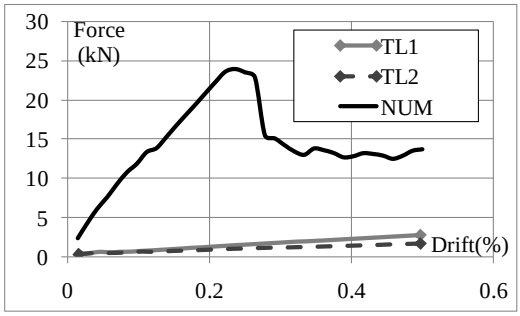

Fig.14: load-displacement diagrams for TL specimens

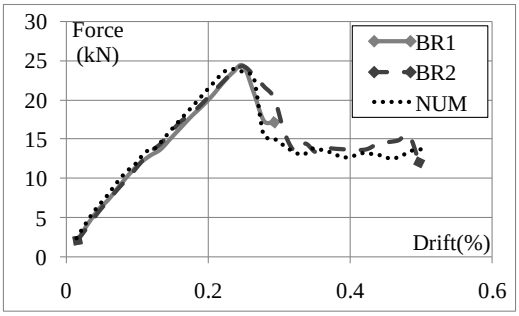

Fig.16: load-displacement diagrams for BR specimens

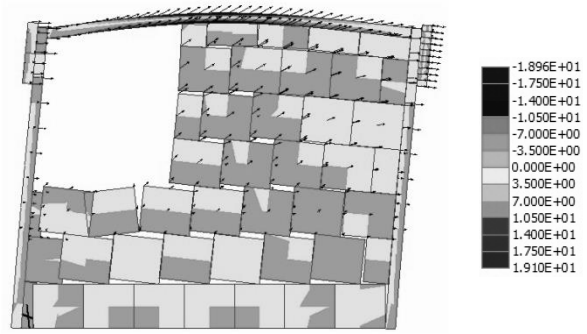

Fig.15: Tensile contours (MPa), Crack patterns and deformed geometry of top - left opening infilled wall (TL 2)

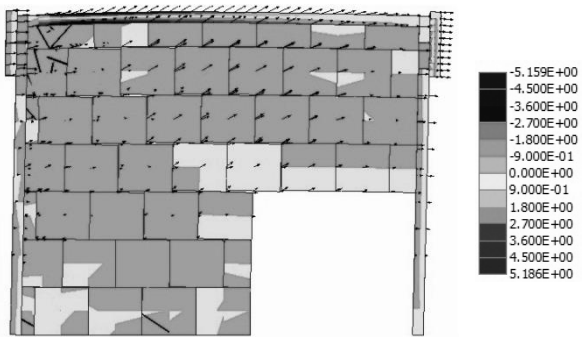

Fig. 17: Tensile contours (MPa), Crack patterns and deformed geometry of bottom-right opening infilled wall (BR 2)

4.3. Opening at the bottom-right corner (BR)

Symbol and properties of the specimens with opening at the bottom-right of the infill is presented in Table 8. Fig.16 shows the load-displacement diagrams for BR specimens and the specimen without opening. According to the results, the opening at the corner does not affect the stiffness and strength of the wall. The opening at the bottom- right corner causes failure of bricks shortly after reaching the maximum strength. Fig. 17 show crack patterns and deformed geometry of BR 2 specimen.

4.4. Opening at the top-right corner (TR)

Table 9 represents the symbol and properties of the specimens with opening at the top-right of the infill. Fig.18 shows load-displacement diagrams for TR specimens. The opening reduces the contact area between the bricks in the corner. With the formation of cracks, there is no factor to resist against the lateral load. As a result, due to the fastening between the bricks, the shear strength of the wall is reduced and wall can be failed under lower loads in comparison with the walls without opening.

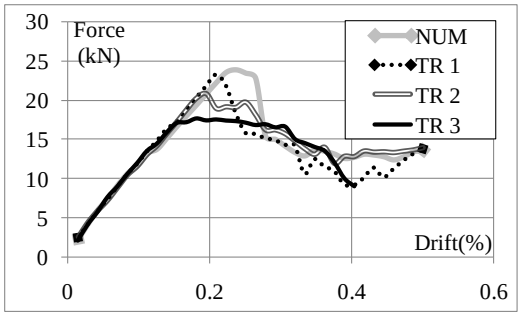

Fig.18: load-displacement diagrams for TR specimens

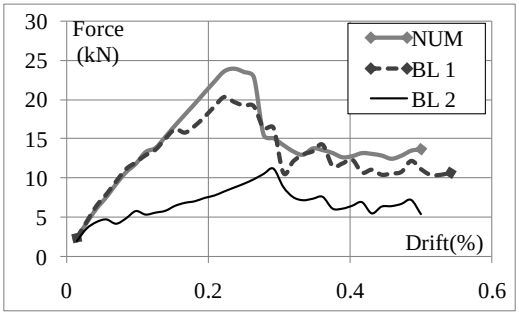

Fig.19: load-displacement diagrams for BL specimens

4.5. Opening at the bottom-left corner (BL)

Symbol and properties of the specimens with opening at the bottom-right of the infill is presented in Table 10. Fig. 19 shows load-displacement diagram for two BL specimens. In this case, the opening reduces the contact area between the bricks. As a result, the shear strength of the wall due to the fastening between the bricks is reduced and the wall destroyed under lower loads than without opening sample.

4.6. The effect of opening shape on wall behavior

To investigate the effect of opening shape on the behavior of the wall, two specimens with dimensions of 50 ×88 cm and 44 ×100 cm with a same opening percentage were selected.

Table 11 lists specimen symbols and properties. Fig.20 show the status of specimens at the time of ultimate loading

Fig.21 shows load-displacement diagrams for specimens with Window and Door openings. The openings reduce the contact area between the bricks in the center of the walls. As a result, the shear strength of the walls is reduced.

According to above equation, the opening reduces the cross-section area and moment of inertia of the wall. As a result, the total stiffness of the wall is reduced with increasing the denominator. It should be noted that the opening length has a greater impact on the stiffness of infills rather than other dimensions. Thus, the stiffness of specimen with Window opening is lower than that of Door opening.

Table 8. Properties of specimens with opening at the bottom-right of the infill (BR)

Specimen Symbol	Infill Dimensions (cm)	Opening Dimensions (cm)	Opening Dimensions ratio	Opening Percentage (%)
BR 1	181×137	50×44	1.25	8.87
BR 2	181×137	75×66	1.13	20

Table 9. Properties of specimens with opening at the top-right of the infill (TR)

Specimen Symbol	Infill Dimensions (cm)	Opening Dimensions (cm)	Opening Dimensions ratio	Opening Percentage (%)
TR 1	181×137	50×55	1.1	11
TR 2	181×137	75×77	1.03	23.27
TR 3	181×137	100×99	1.01	40

Table 10. Properties of specimens with opening at the bottom-left of the infill (BL)

Specimen Symbol	Infill Dimensions (cm)	Opening Dimensions (cm)	Opening Dimensions ratio	Opening Percentage (%)
BL 1	181×137	44×44	1	7.8
BL 2	181×137	56×66	1.17	15

Table 11 Properties of Door and Windows opening infilled wall specimens

Specimen Symbol	Infill Dimensions (cm)	Opening Dimensions (cm)	Opening Dimensions ratio
Door	181×137	44×100	17.7
Window	181×137	88×50	17.7

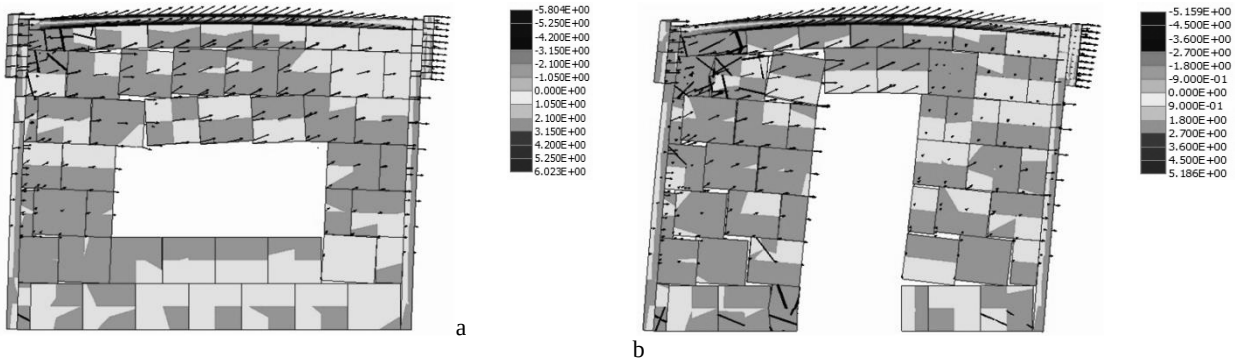

a b

Fig.20: Tensile contours (MPa), crack patterns and deformed geometry of specimens with Window (a) and Door (b) opening

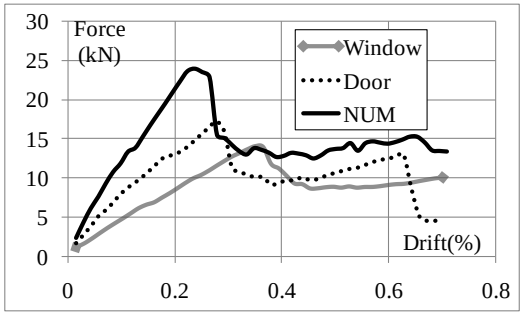

Fig.21: load-displacement diagrams for window and Door opening infilled wall specimens

5. The effect of L-shaped angles on strength and stiffness of infills

L shaped strengthening uses in infilled reinforced concrete and steel frames to reinforce the wall around the opening. L shaped strengthening usually placed in horizontal or vertical or a combined form inside the wall. In order to investigate the effect of strengthening on opening contained infill two specimens with horizontal and vertical strengthening are considered. Table 12represents the symbol and properties of specimens.

Fig.22, display the location of the L shape strengthening in the two specimens O1 and O2. The load-displacement diagrams of specimens are shown in Fig. 23. As can be seen, angles in both specimens lead to a significant increase in the ultimate strength and ductility of the wall with an opening. An angle acts as an anchor and increases the wall strength. As shown in the following figure, the horizontal angles connect two columns and increase the frame stiffness.

Table 12. Properties of horizontal specimens with horizontal and vertical strengthening

Specimen Symbols	Infilled Dimensions (cm)	Opening Dimensions (cm)	L shape Strengthening Dimensions (cm)	Opening percent (%)
Vertical strengthening (O1)	181×137	44×50	10×10×1	8.87
Horizontal strengthening (O2)	181×137	44×50	10×10×1	8.87

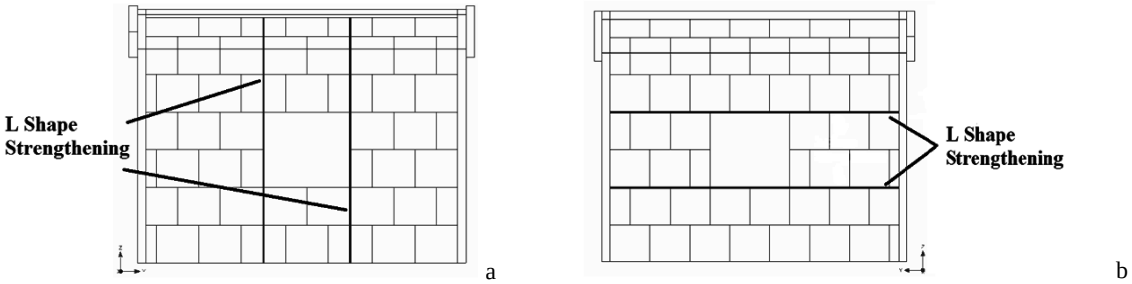

a b

Fig.22: location of the L shape strengthening in the two specimens O1 (a) and O2 (b).

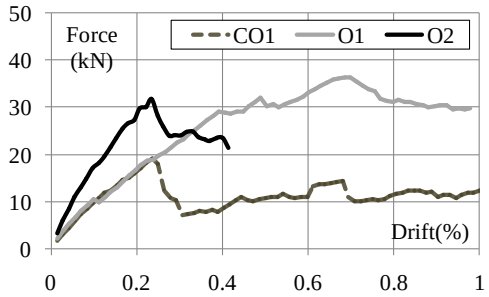

Fig.23: load-displacement diagrams for vertical and horizontal strengthening infills

6. Conclusions

Numerical model of HCT infilled walls based on experimental data have modeled and calibrated in ATENA to investigate the effect of existence of opening on the behavior of infilled walls. Results showed that existing of openings in the top of the wall has the most reduction effect on the strength and stiffness. This is due to inability of the system to transfer the load flow to the wall. The presence of opening in the middle rang of the wall reduces the strength and stiffness too and this reduction depends on the opening area ratio. Presence of the 35% opening, reduce 45% of the strength. Reduction in the walls stiffness depends on the length of the opening and changes in the height of the opening has not significant effect on the stiffness and strength of the wall. Existing of opening in the bottom of the wall and opposite side of load application point has no significant effect on the behavior of the wall. While effect of bottom opening that placed in the side of the load application point on wall behavior, depends on the area ratio of the opening. The strengthening wall with steel L shaped angels can improve the behavior significantly. Horizontal strengthening enhances the stiffness and strength simultaneously while vertical strengthening increases only the strength of the wall with central opening.

7. References

[1] Khanmohammadi, M., Farvili, A. (2011). "Experimental and analytical assessment of performance criteria for partition walls of ordinary buildings." M.Sc. Dissertation, University of Tehran, Tehran, Iran [in Farsi].

[2] Mohammadi, M., Nikfar, F. (2012). "Strength and stiffness of masonry-infilled frames with central openings based on experimental results." Journal of Structural Engineering, Vol. 139(6), pp. 974-984.

[3] Tasnimi, A. A., Mohebkhah, A. (2011). "Investigation on the behavior of brick-infilled steel frames with openings, experimental and analytical approaches." Engineering Structures, Vol. 33(3), pp. 968-980.

[4] Moghaddam, H. A. (2004). "Lateral load behavior of masonry infilled steel frames with repair and retrofit." Journal of structural engineering, Vol. 130(1), pp. 56-63.

[5] Moghadam, H. A., Mohammadi, M. G., Ghaemian, M. (2006). "Experimental and analytical investigation into crack strength determination of infilled steel frames." Journal of Constructional Steel Research, Vol. 62(12), pp. 1341-1352.

[6] Doudoumis, I. N. (2007). "Finite element modeling and investigation of the behavior of elastic infilled frames under monotonic

loading." Engineering Structures, Vol 29(6), pp. 1004-1024.

[7] Koutromanos, I., Stavridis, A., Shing, P. B., Willam, K. (2011). "Numerical modeling of masonry-infilled RC frames subjected to seismic loads." Computers & Structures, Vol. 89(11), pp. 1026-1037.

[8] Markulak, D., Radić, I., Sigmund, V. (2013). "Cyclic testing of single bay steel frames with various types of masonry infill." Engineering Structures, Vol. 51, pp. 267-277.

[9] Jazany, R. A., Hajirasouliha, I., Farshchi, H. (2013). "Influence of masonry infill on the seismic performance of concentrically braced frames." Journal of Constructional Steel Research, Vol 88, pp.150-163.

[10] Fiore, A., Netti, A., Monaco, P. (2012). "The influence of masonry infill on the seismic behavior of RC frame buildings." Engineering Structures, Vol 44 pp. 133-145.

[11] Mosalam KM, White RN, Gergely P. (1997). Static response of infilled frames using quasi-static experimentation1997. Journal of Structural Engineering, Vol. 123(11), pp. 1462–4196.

[12] Al-Chaar, G., Lamb, G. E., Issa, M. A. (2003). "Effect of Openings on Structural Performance of Unreinforced Masonry Infilled Frames." ACI Special Publication, Vol. 211, pp. 247-262.

[13] Liu, Y., Manesh, P. (2013). "Concrete masonry infilled steel frames subjected to combined in-plane lateral and axial loading–Engineering Structures, Vol. 52, pp. 331-339.

[14] Kakaletsis, D., Karayannis, C. G. (2007). "Experimental investigation of infilled R/C frames with eccentric openings." Structural Engineering and Mechanics, Vol 26(3), pp. 231-250.

[15] Kakaletsis, D. J., Karayannis, C. G. (2009). "Experimental investigation of infilled reinforced concrete frames with openings." ACI Structural Journal, Vol, 106(2) pp. 132-141.

[16] Chen, X., Liu, Y. (2015). "Numerical study of in-plane behavior and strength of concrete masonry infills with openings." Engineering Structures, Vol 82, pp. 226-235.

[17] Mallick, D. V., Garg, R. P. (1971). "Effect of openings on the lateral stiffness of infilled frames." Proceedings of the Institution of Civil Engineers, Vol. 49(2), pp.193-209.

[18] Cervenka, V., Cervenka, J., Pukl, R. (2002). "ATENA—a tool for engineering analysis of fracture in concrete." Sadhana, Vol. 27(4), pp. 485-492.

[19] Cervenka, V., Jendele, L., Cervenka, J. (2007). "Atena theory." Praha, Czech Republic.

[20] Kupfer, H., Hilsdorf, H. K., & Rusch, H. (1969). "Behavior of concrete under biaxial stresses." Journal Proceedings, Vol. 66, No. 8, pp. 656-666.

[21] Hordijk, D.A. (1991). "Local Approach to Fatigue of Concrete." TU Delft, Delft University of Technology, Delft, Netherlands.

[22] Mohebkhah, A., Tasnimi, A. A., Moghadam, H. A. (2008). "Nonlinear analysis of masonry-infilled steel frames with openings using discrete element method." Journal of constructional steel research, Vol. 64(12), pp. 1463-1472.

[23] American Society of Civil Engineers, & United States. Federal Emergency Management Agency. (2000). "Global topics report on the prestandard and commentary for the seismic rehabilitation of buildings." The Agency. Washington DC, United States of America.